DOI: 10.15480/882.9353

Eighth International Symposium on Marine Propulsors
smp'24, Berlin, Germany, March 2024

Effect of Model-Structural Dynamics on Propeller-Induced Hull Pressure Measurements

Alireza Jahanbakhsh[1], Emre Cilkaya[1], Lorenzo Moro[1], Heather Peng[1], Mohammed Islam[2]

[1] Department of Ocean and Naval Architectural Engineering, Memorial University of Newfoundland, St. John's, Newfoundland, Canada

[2] Ocean, Coastal, and River Engineering Research Centre, National Research Council Canada (NRC), St. John's, Newfoundland, Canada

ABSTRACT

Propellers are important sources of ship vibrations. Experimental model tests in tow-tank facilities are established methods to assess the design of propellers and ship hulls. However, during these tests, the ship model structural dynamics may affect the results when measuring the propeller-induced hull pressure pulses.

This paper presents the results of towing tests on a scaled model of a bulk carrier at the atmospheric towing tank at NRC-OCRE combined with Operational Deflection Shape Analysis (ODS) of the model's structures. The model was equipped with a four-blade fixed-pitch propeller. Twelve pressure sensors and two sets of eight accelerometers measured propeller-induced pressures and vibrations during the tests. Further, an Experimental Modal Analysis (EMA) identified the model's natural frequencies and mode shapes. The towing tests were performed at different model hull speeds (Vm) and propeller speeds. The signals acquired were post-processed in MATLAB® to find the pressure amplitudes, perform an ODS, assess the structural dynamics, and check possible resonances.

The results indicate that although the local plating does not resonate with the exciting pressure pulsations, the model structure has global modes in the frequency range of interest.

Keywords

Propeller-induced hull pressures, scaled model, tow tank tests, experimental modal analysis, operational deflection shape analysis

1 INTRODUCTION

Propellers are the main sources of ship vibrations, which may affect onboard comfort and the health of crew members. Over the last few decades, researchers have developed experimental full-scale or model-scale measurements to validate numerical simulations, develop empirical formulas to estimate propeller-induced hull pressures, and provide ship designers with design tools to mitigate propeller-induced hull pressures.

In 1981, Holden et al. (1981) presented empirical formulations to compute pressure fluctuations for both non-cavitating and cavitating propellers. This method considers the geometrical and hydrodynamic characteristics of propellers. They were developed based on the analysis of experimental data acquired in the late 70s on a series of merchant vessels. These formulations have been used as a preliminary tool to estimate propeller-induced hull pressures in the early design phases of new vessels. Since then, few papers have presented the analysis of propeller-induced hull pressures from full-scale data. Choi et al. (2004) presented a method to estimate cavitation-induced forces on the hull of a container vessel, and Zambon et al. (2019, 2021) conducted full-scale acceleration measurements and Finite Element simulations to validate the use of the Holden Method (HM) to the case of a superyacht. Their study revealed that HM tends to overestimate propeller-induced pressure. They also studied the vibration response of their FE model to the experimentally validated HM-based forces in different phase offsets.

Other studies have focused more on the use of onboard vibration and pressure measurements to estimate Underwater Radiated Noise (URN) (Turkmen et al. 2017), (Lee et al. 2014).

The need for design methods to estimate propeller-induced hull pressures has led to the development of model tests conducted in towing tank facilities. When these tests are

conducted to measure propeller-induced pressure pulses on the hull stern of ship models, the experimental results may be affected by the ship model structural dynamics.

The impact of the model's structural response to the hydrodynamic measurements has been explored mainly in the study of wave-induced structural loads. The International Towing Tank Conference (ITTC) has presented procedures and guidelines to study global loads through model testing (ITTC 2017). Maron & Kapsenberg (2014) devised a model of a large container ship that aims to emulate the flexible behavior of the ship's hull structure. Houtani et al. (2018) introduced a hydro-elastic design for a container ship model to assess its response to wave-induced bending and torsional vibrations. Jiao et al. (2016) introduced a segmented large-scale hydrodynamic model, conducting measurements during sea trials while the model operated independently with its propulsion system. They validated their method by comparing their measurements with numerical and lab-scale data.

Few studies have been conducted on the effect of the model's structural dynamics on the measurements of propeller-induced hull pressures in lab facilities. Tani et al. (2017) emphasized the importance of considering the structural resonance properties of the mounting plate when investigating pressure fluctuations and noise resulting from cavitation during experiments in cavitation tunnels.

More notably, Van Wijgaarden (2011) conducted a series of experimental tests to verify the effect of the model's structural dynamics on the measurements of propeller-induced hull pressures. Following the ITTC committee's suggestion to include vibration measurements with hull pressure assessments (ITTC 2002) and (ITTC 2008), they incorporated the model's structural response in their studies. To address the impact of vibration-induced pressures (VIPs), they measured propeller-induced pressures and evaluated the aftship response to shaker and propeller excitations using accelerometer data. Later, they used a Boundary Element Method (BEM) code to identify VIPs and adjust the measured pressures. As an example, they found that the error caused by VIPs in measuring the normalized 1st Blade Passing Frequency (BPF) harmonic for a single propeller at two different shaft RPMs equal to 34% and 17%.

Building on Van Wijngaarden's study, this paper presents a series of experimental tests performed to evaluate the structural dynamic response of a scaled ship model during tests performed to measure propeller-induced pressure signals. During the tests, concurrently with pressure signals, we performed Operational Deflection Shapes (ODS) analysis to study model dynamics. Besides, the dynamic characteristics of the model in dry and wet conditions were found through EMA and analytical approximations. By combining pressure data with the structural dynamic analysis, we find whether the natural frequencies of the model fall in the frequency range of interest and, thus, if the model's dynamic may affect the pressure measurements. This is the first phase of a larger project that aims to understand propeller-induced hull pressures, hull vibration and underwater noise through towing tank tests.

Section 2 outlines the methodology used in this study, encompassing measurements, signal processing, and analytical techniques employed. Section 3 presents the relevant results based on the research methodology. This paper introduces a technique to assess potential resonances by focusing on the structural response in towing tests. The approach involves incorporating vibration measurements and signal processing to emphasize the significance of structural behavior. Specifically, the method aims to detect resonances while measuring pressure amplitudes, underscoring the importance of this aspect in the testing process.

2 METHODOLOGY

In this study, we conducted towing tests on a scaled ship model, focusing on the pressure and acceleration signals generated by propeller rotations. After measuring and processing these signals, we found the pressure distribution on the aftship surface of the model. Additionally, we utilized Operational Deflection Shapes (ODS) to assess the response of the ship structure both at the sensors's position aftship and globally along the model's deck.

The natural frequencies of both the plate and the model were determined to identify potential resonances. The plate exhibited sufficient stiffness, placing its first natural frequency outside the frequency range of interest (i.e., below 100 Hz). We used the modal analysis (hammer test) in dry conditions to find the model's natural frequencies and employed an analytical formula to account for added mass effects. Ultimately, these findings were integrated to establish a comprehensive procedure for considering the dynamic characteristics of the model structure in hydrodynamic tests.

2.1 Experimental measurements

2.1.1 Scaled model and the propeller

The tested model (Figure 1) is a scaled post-Panamax bulk career with the dimensions listed in Table 1. The model's propeller, featuring a fixed-pitch four-bladed design, had a modified NACA section profile (Table 2) to guarantee non-cavitating conditions. Figure 2 illustrates the configuration of the propeller mounted on the model.

Table 1- Scaled Ship Model and Real Ship Dimensions

Dimensions [m]	Model	Ship
Length Overall [m]	7.142	226
Breadth [m]	1.02	32.25
Depth[m]	0.623	19.75
Draft[m]	0.43	13.5
Displacement [t]	2.685	85637

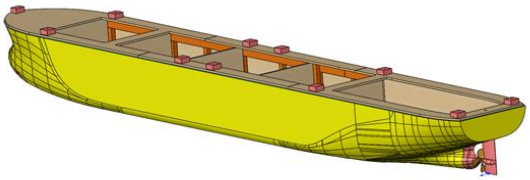

Figure 1- 3D configuration of the model

Figure 2- Propeller mounted aftship of the model

Table 2- Propeller properties

Property	Values
Diameter [m]	0.235
Number of Blades	4
Pitch/Diameter (P/D) distribution	1.1 (constant)
Expanded Area Ration (EAR)	0.65
Section Profile	modified NACA 66
Material	Copper

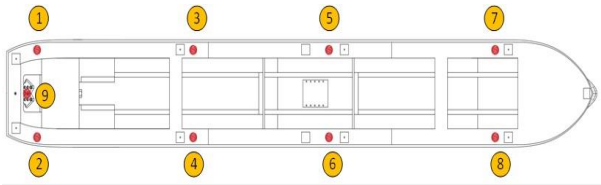

Figure 3- Global arrangement of the accelerometers

2.1.2 Model tests

Towing tests, containing resistance, self propulsion (SP), and bollard pull (BP) tests, were conducted at the towing tank of the Ocean, Coastal, and River Engineering Research Centre, National Research Council Canada (NRC-OCRE) in St. John's, NL, Canada. The towing tank is 200 meters long, 12 meters wide, and 7 meters deep. We explored various combinations of shaft rotation and model speeds, as outlined in Table 3.

The propeller was mounted on the model during the SP and BP tests. A conical faired hub was installed during the resistance tests to ensure smooth flow over the shaft. This way, the propeller and shafting inertial effects were considered in the test with and without the propeller.

Table 3-Towing tests scheduling

Model speed [m/s]	Shaft rotation speed [RPS]
Resistance and SP test	SP and BP test
1.15	4.5
1.468	6
1.95	7
	9
	10.1
	11

2.2 Experimental Modal Analysis (EMA)

Experimental Modal Analyses (EMA) were performed using a Single Input Multi Output (SIMO) system to assess the dynamics of the model. The excitation was applied by a PCB-instrumented piezoelectric hammer, model 086C03, as the Single Input. PCB piezoelectric accelerometers, model 352C33 (one as the reference), were installed on the model's deck to measure the response, as depicted in Figure 3. The measurement data was collected by NI DAQ, model 9234, cards and converted into digital signals for post-processing. The scaled ship model was suspended from the OEB crane using a strong back and two lifting slings to achieve the free-free boundary condition (Figure 4). The slings' natural frequencies were found to be significantly lower than the model's first natural frequency, thus not impacting its measured dynamic characteristics. Figure 5 illustrates the hammer used in the test and one accelerometer mounted on the model's deck.

2.3 Signal Processing

The acquired data was post-processed using MATLAB® codes developed to calculate the acceleration frequency response functions (FRFs). The coherence functions of the acquired signals were calculated to assess the correlation between input and output signals and the quality of the tests. For the hammer test, three impacts were applied, and the FRFs were averaged.

FRFs were also calculated during towing tank tests. The ABRAVIBE MATLAB® toolbox was used to perform the ODS analysis for both global and local arrangements; accelerometer No. 9, shown in Figure 6, was set as the reference.

Figure 4-Hammer test on the scaled model structure

(a) (b)

Figure 5-EMA instrument, (a) hammer, (b) accelerometer mounted on the model

2.4 Added mass effect

We implemented the analytical formula proposed by Lewis—Equation (1)—to evaluate the effect of added mass on the hull structural response (Korotkin 2009). Considering $B/2T \cong 1.2$, we calculated the added mass per length according to Equation (2) and used the block coefficient of the ship, $C_B = 0.85$, to adjust the effective length for the added mass. Considering the calculated added mass, we found the model's wet natural frequencies based on Equation (3) as presented in (Pais 2018).

$$k_{33} = \frac{\lambda_{33}}{(\pi/2)\,\rho\,(B/2)^2} \tag{1}$$

$$\lambda_{33} = 494 \times l \times C_B = 2998\ \text{kg} \tag{2}$$

$$\lambda_{33} = \Delta \left[\left(\frac{\omega_{n,dry}}{\omega_{n,wet}} \right)^2 - 1 \right] \tag{3}$$

Where λ_{33} is the added mass of the ship in the vertical direction, k_{33} is its coefficient, Δ is the ship displacement, C_B is the block coefficient, and $\omega_{n,dry}$ and $\omega_{n,wet}$ are the natural frequencies in dry and wet conditions, respectively.

2.5 Local plate

As illustrated in Figure 6, the local accelerometers and pressure sensors were mounted on a polyurethane plate, the main dimensions of which are listed in Table 4. We conducted an FE modal analysis to assess its natural frequencies.

Table 4: Geometrical properties of the polyurethane plate

Parameter	Value
Length [mm]	310
Width [mm]	200
Thickness [mm]	50
density [kg/m^3]	550
Elastic modulus [MPa]	731

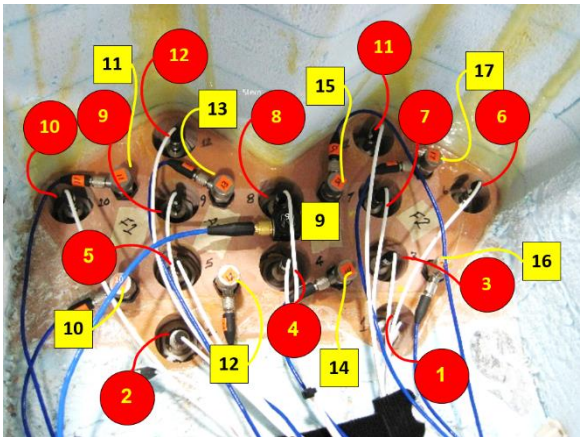

Figure 6- Arrangement of the local accelerometers (yellow boxes) and pressure sensors (red circles)

3 RESULTS

3.1 Propeller-induced pressures

Figure 7 shows the amplitudes of all pressure signals measured during the BP test (Vm=0 m/s) at the shaft rotation speed of 4.5 RPS. Figure 8 and Figure 9 illustrate the vector and contour representations of pressure amplitudes at the sensor locations under identical conditions. Figure 10 displays pressure amplitudes obtained from a single sensor (P1) across six shaft rotation and four model speeds, enabling a comprehensive comparison. It also shows that the pressure amplitudes in the BP tests are always higher than in the SP tests. We followed this finding and considered the BP tests in our consequent considerations as the worst-case scenario.

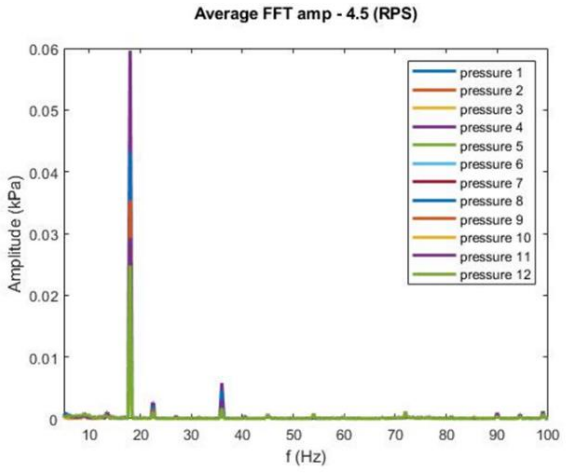

Figure 7-Pressure amplitudes, Vm=0 m/s, and 4.5 RPS

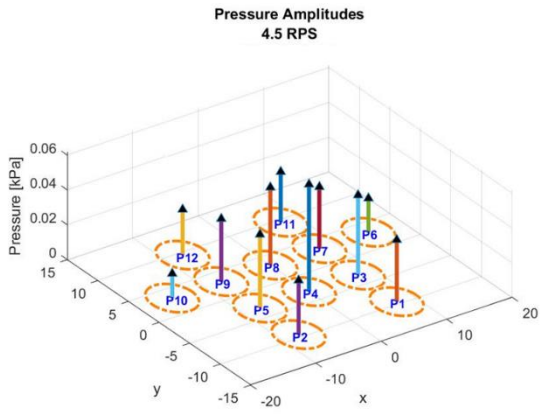

Figure 8-Vectors of pressure amplitudes, Vm=0 m/s, and 4.5 RPS

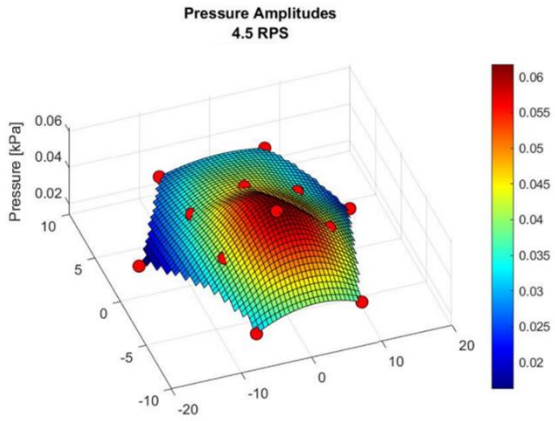

Figure 9-Contour plot of pressure amplitudes, Vm=0 m/s, and 4.5 RPS

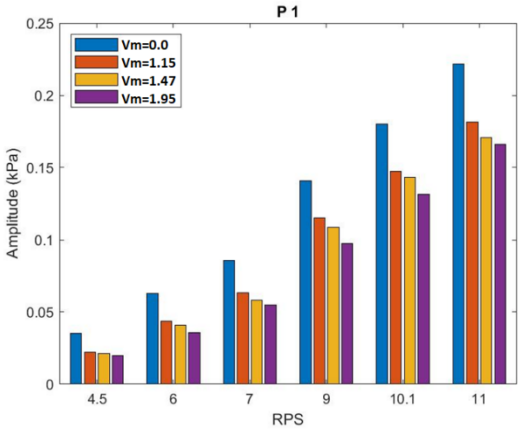

Figure 10- Pressure amplitudes obtained from a single sensor (P1) across six shaft rotation speeds and four model speeds

3.2 Accelerations and ODS

3.2.1 SP and BP tests

The acceleration signals were analyzed, and amplitudes were calculated for both local and global accelerometers in each test scenario (Figure 11). In addition, acceleration spectrums were calculated to analyze 1) the acceleration amplitudes and 2) the structural behavior of the model and plate using Operational Deflection Shapes (ODS). Figure 12 shows the model and local plate deformations in the BP test at the shaft rotation speed of 4.5 RPS.

3.2.2 Resistance tests

The Resistance tests were carried out under the specified conditions outlined in Section 2.1.2, involving the conical faired hub. Figure 13 and Figure 14 show the 1st torsional and 1st bending modes of the model excited during the resistance tests at model speeds of 1.15 and 1.95 m/s and shaft rotation speeds equal to 6 and 11 RPS. Table 5 and Table 6 outline the 1st torsional and 1st bending modes obtained through ODS.

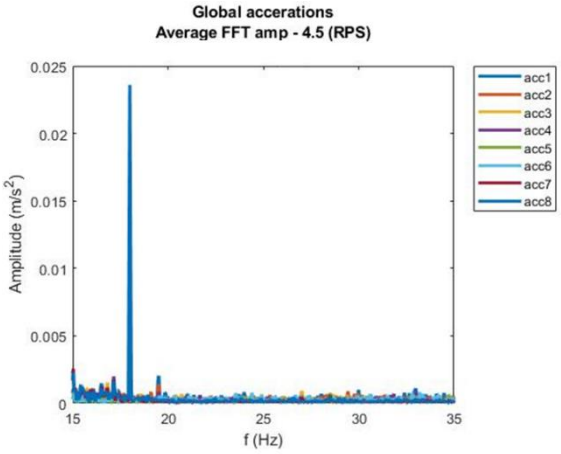

(a)

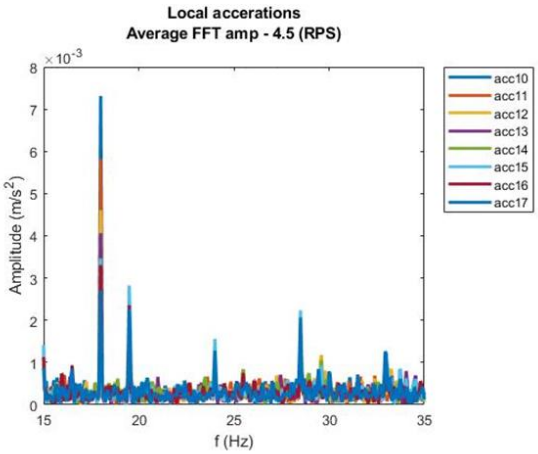

(b)

Figure 11-Acceleration amplitudes in Vm=0.0 m/s, and 4.5 RPS: (a) global, (b) local

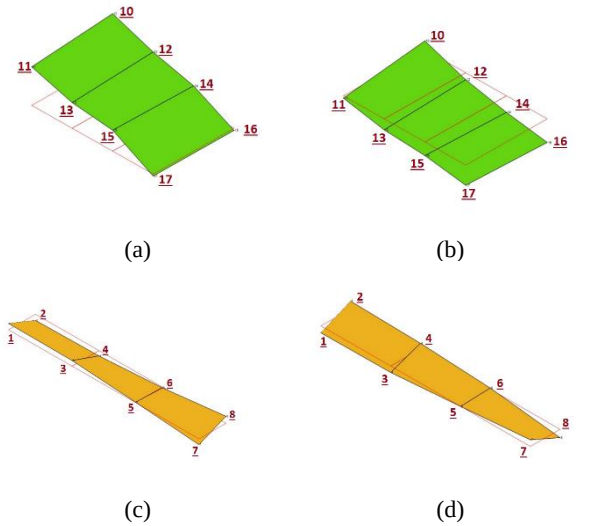

(a) (b)

(c) (d)

Figure 12-Deformation (1st harmonic) in Vm=0.0 m/s, and 4.5 RPS: (a & b) local plate, (c & d) global model

Table 5. Natural frequencies obtained from experimental tests (ODS)-mode 1

Natural frequency - 1st torsional mode	
Res., Vm=1.15 m/s, 6 RPS	11.8 Hz
Res., Vm=1.15 m/s, 11 RPS	11.0 Hz
Res., Vm=1.95 m/s, 6 RPS	11.8 Hz
Res., Vm=1.95 m/s, 11 RPS	11.0 Hz

Table 6. Natural frequencies obtained from experimental tests (ODS)-mode 2

Natural frequency - 1st bending mode	
Res., Vm=1.15 m/s, 6 RPS	24.1 Hz
Res., Vm=1.15 m/s, 11 RPS	22.1 Hz
Res., Vm=1.95 m/s, 6 RPS	24.1 Hz
Res., Vm=1.95 m/s, 11 RPS	22.1 Hz

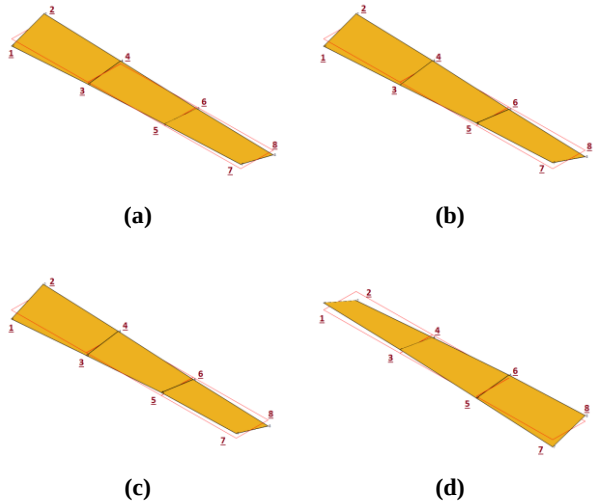

(a) (b)

(c) (d)

Figure 13. 1st torsional mode excited through Resistance tests, (a) Vm=1.15 m/s, 6 RPS, (b) Vm=1.15 m/s, 11 RPS, (c) Vm=1.95 m/s, 6 RPS, and (d) Vm=1.95 m/s, 11 RPS

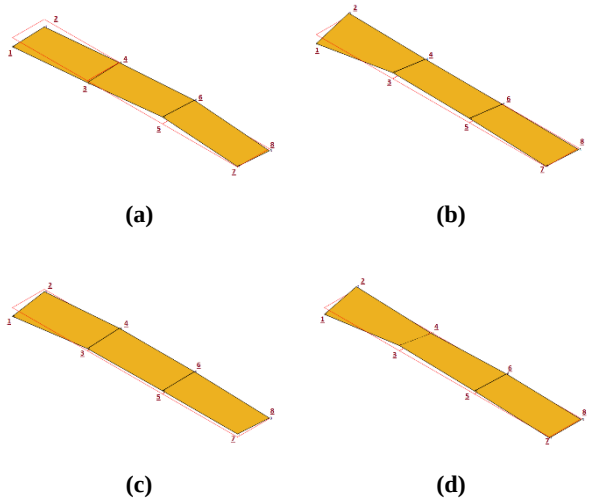

(a) (b)

(c) (d)

Figure 14. 1st bending mode excited through Resistance tests, (a) Vm=1.15 m/s, 6 RPS, (b) Vm=1.15 m/s, 11 RPS, (c) Vm=1.95 m/s, 6 RPS, and (d) Vm=1.95 m/s, 11 RPS

3.3 Experimental Modal Analysis (EMA)

The model's dynamic characteristics under dry conditions were determined experimentally using EMA and hammer testing. In Figure 15, accelerance amplitude plots are shown for accelerometers positioned on the model's deck, revealing the identification of its first torsional and first and second bending modes. An example of this analysis is presented in Figure 16, showcasing accelerance amplitude, phase, and coherence data for accelerometer No. 3. Notably, the coherence near natural frequencies is close to one, indicating reliable measurements, as shown in the figure. Figure 17 shows the 1st torsional and 1st bending modes of the scaled ship model measured through EMA.

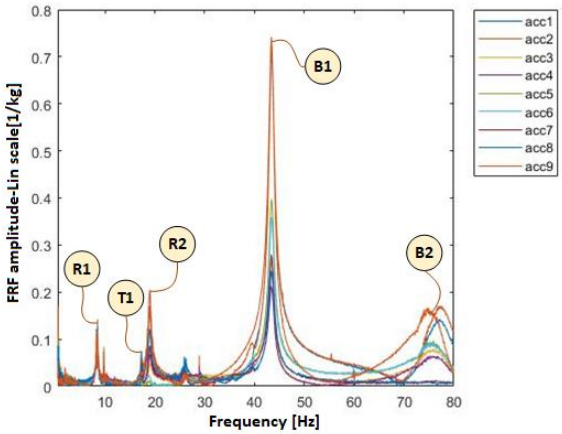

Figure 15-FRFs (accelerance) amplitudes from EMA

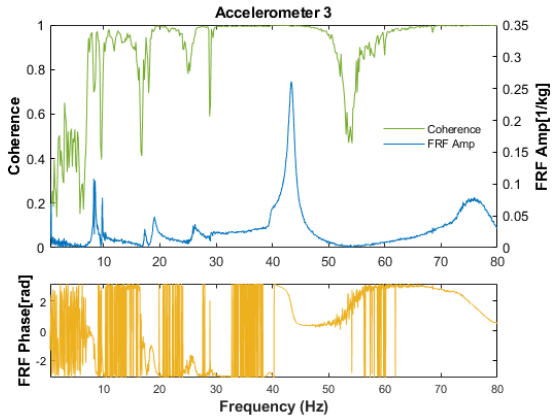

Figure 16- FRF (accelerance) amplitude and phase and the relevant coherence for accelerometer 3

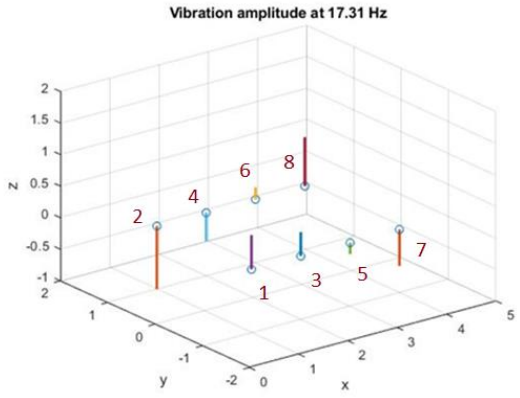

(a)

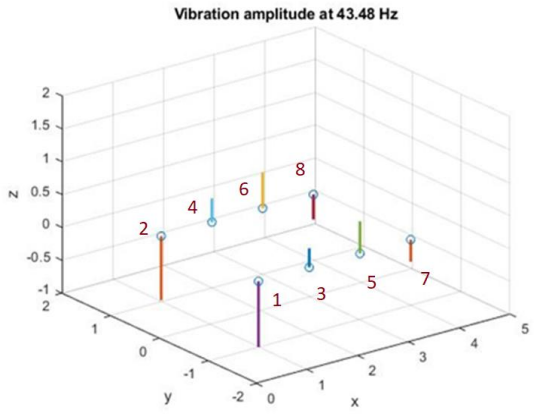

(b)

Figure 17-EMA captured modes, (a) 1st torsional and (b) 1st bending

3.4 Analytical results

The hammer test was conducted on the model without the ballast weights necessary in water. We used these natural frequencies and updated the FE model of the scaled ship in a separate phase of our research. The updated FE model, equipped with the ballast weights, is implemented to calculate the dry natural frequencies mentioned in Equation (3). Therefore, the values of dry natural frequencies listed in Table 7 are less than those presented in Figure 17 due to the additional ballast weights.

Table 7 presents the results of the dry and wet natural frequencies of the ship model calculated according to Section 2.4.

Table 7- Natural frequencies of the scaled ship model

Mode number	Natural frequency [Hz]		Type of mode
	Dry with ballast weights	Wet	
1	14.64	10.06	1st torsional
2	22.67	15.58	lateral bending
3	36.18	24.85	1st bending

3.5 Dynamic characteristics of the plate

Figure 18 depicts the 1st torsional and 1st bending modes of the polyurethane plate obtained through a FE simulation. None of the plate's normal modes fall within the frequency range of interest in this study; thus, no significant resonance and vibration-induced pressures are generated.

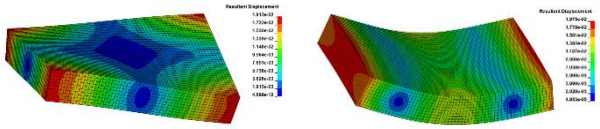

(a) (b)

Figure 18-Normal modes of the local plate, (a) 489 Hz and (b) 541 Hz

4 DISCUSSION

The primary objective of the tests was to measure the propeller-induced pressures aftship of the model. By analyzing the pressure data, the following are found:

- It is determined that the propeller operates without cavitation, indicated by distinct peaks at the first and second harmonics for all pressure sensors, as shown in Figure 7. The absence of pressure spectra across a wide range of frequencies, confirmed by the pressure plots, supports the non-cavitating condition. This observation also applies to the induced acceleration signals, as depicted in Figure 11.
- Variations in pressure amplitudes are observed among different sensors, with a specific sensor located above the propeller registering the highest pressure. This maximum pressure amplitude at sensor P4 (No. 4) is evident in the vector representation displayed in Figure 8.
- Figure 9 provides a contour representation of pressure amplitudes, with the red spot indicating the area of maximum pressure. Integrating the pressure distribution over the actual surface is crucial to accurately determining the propeller excitation force.

- Figure 10 shows that the BP tests lead to the highest induced pressure amplitudes among the pressures obtained from various model and shaft rotation speeds. It marks this condition as the critical worst-case scenario for design considerations.

The non-rigid nature of the model can affect the measured pressure amplitudes, as also mentioned in (Wijngaarden 2011), depending on its dynamic characteristics.

The results from EMA, along with the analytically calculated wet natural frequencies of the model, confirm that these natural frequencies are in the frequency range of interest in this research (i.e., below 100 Hz), which increases the chance of resonance for such experiments.

In the case presented here, the non-cavitating working conditions of the propeller entail that the effect of pressure pulses on the structural response of the model is limited when the excitation frequency is different from the structural wet natural frequency. However, there is no guarantee to prevent this resonance as different hydrodynamic conditions (RPS and Vm) will result in different excitation frequencies. In other words, changes in the propeller or model speeds may result in the resonance provided that the natural frequencies are in the range.

Operational Deflection Shape (ODS) analyses show the structural response throughout the towing tank experiments. During the resistance tests, the 1st torsional and 1st bending modes of the model were excited (Table 5 and Table 6), and the outcomes exhibited strong alignment with the analytical results presented in Table 7.

The results from FE analysis of the local plate reveal that its deformation has a minimal impact on the measured pressures. This is because its lowest natural frequency falls far outside the frequency range of interest. Consequently, in this case, it is only necessary to consider global resonances when analyzing pressure fluctuations caused by vibrations. Also, the assumption of a nondeformable plate for further vibroacoustic analyses is reasonable.

5 CONCLUSIONS

It can be inferred that the model's dynamics may lead to vibrations impacting the measured pressures in hydrodynamic tests and that ODS analyses help prevent facing the resonance phenomenon prior to conducting towing tank tests for recording propeller-induced hull pressure.

In our case study, no resonance occurred during the tests we conducted. Nonetheless, the damped model's modes may affect the pressure measurements. In addition, as the natural frequencies fall in the frequency range of interest, resonance may happen with a variation of model speed or propeller shaft speed. While the tests were performed for a non-cavitating propeller, the results of this study are also relevant for cavitating propellers, whose pressure spectra show broad-band excitations.

The modified pressures obtained from these simulations will be used in the subsequent phases of this research project to validate Computational Fluid Dynamics (CFD) simulations.

ACKNOWLEDGMENT

This study is part of the "Propeller Induced Noise and Vibration (PINOV)" project funded by Transport Canada, National Research Council of Canada, and the Department of Industry, Energy and Technology (IET) of the Government of Newfoundland and Labrador, Canada.

REFERENCES

Choi, G., Lee, J., & Kim, H., (2004). Estimation of cavitation induced fluctuating forces on the hull for large container carriers, in: Proceedings of the 9th Symposium on Practical Design of Ships and Other Floating Structures. pp. 562–567.

Holden, K.O., Fagerjord, O., & Frostad, R., (1981). Early Design-Stage Approach To Reducing Hull Surface Forces Due To Propeller Cavitation. Transactions - Society of Naval Architects and Marine Engineers **88**, 403–442.

Houtani, H., Komoriyama, Y., Matsui, S., Oka, M., Sawada, H., Tanaka, Y., & Tanizawa, K., (2018). Designing a hydro-structural model ship to experimentally measure its vertical-bending and torshional vibrations. Journal of Advanced Research in Ocean Engineering **4**, 174–184.

ITTC, (2017). Global Loads Seakeeping Procedure.

ITTC, (2008). Specialist Committee on Cavitation,Final Report and Recommendations to the 25th ITTC, Proceedings of 25th ITTC – Volume II.

ITTC, (2002). The Specialist Committee on Cavitation Induced Pressures, Final Report and Recommendations to the 23rd ITTC, Proceedings of the 23rd ITTC – Volume II.

Jiao, J., Ren, H., Sun, S., Liu, N., Li, H., & Adenya, C.A., (2016). A state-of-the-art large scale model testing technique for ship hydrodynamics at sea. Ocean Engineering **123**, 174–190.

Korotkin, A.I., (2009). Added Masses of Ship Structures, Fluid Mechanics and Its Applications. Springer Netherlands, Dordrecht.

Lee, J.-H., Park, H.-G., Kim, J.-H., Lee, K.-J., & Seo, J.-S., (2014). Reduction of propeller cavitation induced hull exciting pressure by a reflected wave from air-bubble layer. Ocean Engineering **77**, 23–32.

Maron, A., & Kapsenberg, G., (2014). Design of a ship model for hydro-elastic experiments in waves. International Journal of Naval Architecture and Ocean Engineering **6**, 1130–1147.

Pais, T., (2018). Analytical and numerical computation of added mass in vibration analysis for a superyacht. Ships and Offshore Structures **13**, 443–450.

Tani, G., Villa, D., Gaggero, S., Viviani, M., Ausonio, P., Travi, P., Bizzarri, G., & Serra, F., (2017). Experimental investigation of pressure pulses and radiated noise for

two alternative designs of the propeller of a high-speed craft. Ocean Engineering **132**, 45–69.

Turkmen, S., Aktas, B., Atlar, M., Sasaki, N., Sampson, R., & Shi, W., (2017). On-board measurement techniques to quantify underwater radiated noise level. Ocean Engineering **130**, 166–175.

Wijngaarden, H.C.J. van, (2011). Prediction of propeller-induced hull-pressure fluctuations. Maritime Research Institute Netherlands (MARIN).

Zambon, A., Moro, L., & Biot, M., (2021). Vibration analysis of super-yachts: Validation of the Holden Method and estimation of the structural damping. Marine Structures **75**, 102802.

Zambon, A., Moro, L., & Biot, M., (2019). Effect of propeller phase angles on the vibration response of a twin-screw super-yacht, in: Proceedings of the 26th International Congress on Sound and Vibration, ICSV 2019. Canadian Acoustical Association, pp. 4608–4615.